

Inovações e Soluções Sustentáveis em Engenharia Ambiental

Comparative analysis of methodologies for assessing chlorophyll-a concentration in the Billings Reservoir

Análise comparativa de metodologias para avaliação da concentração de clorofila-a no Reservatório Billings

Brenda Camila Ferreira^I, Tobias Bleninger^I,
Mayra Ishikawa^{II}, José Antônio de Jesus^I,
Laís Amorim^{III}

^IUniversidade Federal do Paraná, PR, Brazil

^{II}Universidade Federal de São Paulo, SP, Brazil

^{III}The Federal Institute of Hydrology, KO, Germany

ABSTRACT

Monitoring chlorophyll-a concentrations (Chl-a) is essential for managing water quality and mitigating eutrophication risks. Traditional in situ monitoring methods often suffer from data gaps, making remote sensing a valuable complementary tool. This study evaluates data from two remote sensing platforms (SNAP and AlgaeMap), the Delft3D hydrodynamic model, and in situ observations (CETESB) to analyze Chl-a in the Billings Reservoir, São Paulo, from 2017 to 2021. Chl-a behavior was assessed under different seasonal conditions. Results show that during the dry season, SNAP and AlgaeMap provided similar Chl-a estimates, though with some quantitative differences, particularly in marginal areas. AlgaeMap produced higher Chl-a concentrations in upstream regions during the rainy season. A 67.13% agreement was observed between SNAP and Delft3D, indicating challenges in aligning modeled and satellite-derived data. SNAP's seasonal sensitivity was stronger, showing improved correlation with CETESB data in the dry season. With Chl-a below 100 µg/l, the correlation strengthened, reaching R^2 values of 0.71 for SNAP and 0.75 for AlgaeMap. The integration of Delft3D provided valuable spatial information, complementing satellite data and capturing temporal dynamics. The combined approach of remote sensing and hydrodynamic modeling enhances the accuracy of Chl-a assessments, offering a comprehensive strategy for reservoir management and eutrophication prevention.

Keywords: Remote sensing; Hydrodynamic modeling; In situ data; Water quality monitoring

RESUMO

O monitoramento da concentração de clorofila-a (Chl-a) é fundamental para a gestão da qualidade da água e mitigação dos riscos de eutrofização. Métodos de monitoramento in situ frequentemente sofrem com lacunas de dados, tornando o sensoriamento remoto (SR) uma ferramenta complementar valiosa. Este estudo avalia dados de Chl-a obtidos por SR (SNAP e AlgaeMap), modelo hidrodinâmico (Delft3D) e observações in situ (CETESB) no Reservatório Billings, São Paulo, de 2017 a 2021. Os resultados mostram que, durante a estação seca, SNAP e AlgaeMap forneceram estimativas semelhantes de Chl-a, embora com algumas diferenças quantitativas, principalmente nas margens. AlgaeMap apresentou concentrações mais altas de Chl-a nas regiões a montante na estação chuvosa. Observou-se uma concordância de 67,13% entre SNAP e Delft3D, indicando desafios na correspondência entre modelagem hidrodinâmica e SR. A sensibilidade sazonal do SNAP foi maior, com melhor correlação com os dados CETESB na estação seca. Considerando Chl-a abaixo de 100 µg/l, a correlação aumentou, alcançando R^2 de 0,71 para SNAP e 0,75 para AlgaeMap. A integração do Delft3D complementou dados de satélite com informações espaciais relevantes. A abordagem combinada das diferentes metodologias aprimora a precisão das avaliações de Chl-a, oferecendo uma estratégia abrangente para gestão de reservatórios e prevenção da eutrofização.

Palavras-chave: Sensoriamento remoto; Modelagem hidrodinâmica; Dados in situ; Monitoramento da qualidade da água

1 INTRODUCTION

Reservoirs play a fundamental role in providing a diverse range of water uses, including drinking water supply, irrigation, hydropower generation, and recreational activities (Jesus 2006). But the indiscriminate exploitation of this vital resource can have significant repercussions on both the volume and quality of water within these systems (Amorim 2020; Gurski et al. 2021).

According to CONAMA Resolution No. 357/2005, it is essential that water quality adheres to specific classifications to safeguard aquatic ecosystems and ensure public health. Traditional monitoring approaches, which often rely on field sampling at discrete points, frequently lack the necessary spatial and temporal representativeness required to capture the dynamic nature of reservoir systems (Barbosa et al. 2019; Gurski et al. 2021; Lobo et al. 2021).

Considering these limitations, remote sensing has emerged as a powerful alternative for the comprehensive spatiotemporal analysis of water bodies (Machado &

Baptista 2016; Neves et al. 2021). Remote sensing technologies facilitate the acquisition of extensive datasets over large areas and varying temporal scales, thereby enhancing our understanding of water quality dynamics (Pompêo et al. 2021; Neves et al. 2021).

By utilizing satellite imagery and other remote sensing tools, researchers can monitor key water quality parameters, identify trends, and detect anomalies that may not be observable through conventional sampling methods (Barbosa, Novo, and Martins 2019; Neves et al. 2021).

Despite its numerous advantages, remote sensing encounters several challenges that can hinder effective monitoring, particularly the frequent occurrence of cloud cover in satellite images (Barbosa, Novo, and Martins 2019), which compromises data acquisition in the study area. Furthermore, the dynamic nature of water bodies can significantly affect the spectral range utilized for water quality assessments, especially in the infrared spectrum (Barbosa, Novo, and Martins 2019).

In their investigations, Pompêo et al. (2021) and Neves et al. (2021) evaluated multiple parameters indicative of water quality, with a particular focus on chlorophyll-a concentration (Chl-a). Utilizing the Sentinel-2 satellite in conjunction with the Sentinel Application Platform (SNAP) software, both studies concluded that this satellite-based approach offers valuable information into water quality dynamics in reservoirs.

Chlorophyll-a is a critical indicator of the health and functioning of aquatic ecosystems. This pigment, essential for photosynthesis in plants, algae, and cyanobacteria, plays a vital role in oxygen production and forms the base of the aquatic food chain (Neves et al. 2021; Pompêo et al. 2021; Gurski et al. 2021). According to Gurski et al. (2021), the monitoring of Chl-a enables the detection of temporal changes in ecosystem health, facilitates the identification of emerging issues, and supports the formulation of effective management strategies to mitigate potential risks.

However, elevated concentrations of chlorophyll-a may indicate a proliferation of algae, raising concerns about potential eutrophication (Amorim 2020). Eutrophication is characterized by the excessive enrichment of water bodies with nutrients, primarily

due to anthropogenic activities, such as the discharge of nitrogen and phosphorus from sewage and agricultural fertilizers (Machado and Baptista 2016). This nutrient overload can stimulate algal blooms, which subsequently lead to various issues, including the degradation of water quality (Gurski et al. 2021).

Comparing methodologies for assessing Chl-a is important, as different methods can yield varied results. This comparison is essential for validating the accuracy and reliability of each method, ensuring the representativeness of the collected data. To evaluate the potential of integrating remote sensing within situ measurements, this study focused on the Billings Reservoir, situated within the sub-basin of the Upper Tietê Basin in the southwestern region of São Paulo Metropolitan Area.

The Billings Reservoir is confronted with significant challenges stemming from pollutant discharges, which have accelerated the process of eutrophication. A notable intervention occurred in 1928 when the flow of the Tietê River was redirected into the Billings Reservoir to mitigate flooding during periods of heavy rainfall (Jesus 2006).

Although, this intervention subsequently began to adversely affect various water quality parameters (Jesus 2006). As highlighted by Jesus (2006) and Amorim (2020), the reservoir is compartmentalized into distinct sections, with the Pedreira area designated for flood control and the Rio Grande section serving primarily for water supply.

In this context, the dam on the Rio Grande plays a crucial role in regulating the exchange of water mass between the Rio Grande Reservoir and the main body of the Billings Reservoir. This study aimed to compare two remote sensing methodologies: (1) the Sentinel Application Platform (SNAP) software and (2) the AlgaeMap application. Additionally, in situ data provided by the Environmental Company of the State of São Paulo (CETESB) were incorporated into the analysis, along with data derived from mathematical modeling using Delft3D software, as reported by Amorim (2020).

This study was conducted from 2017 to 2021, facilitating a comprehensive analysis of three tools: AlgaeMap, SNAP, and Delft3D, in conjunction with field measurements. Given the intricate configuration of the Billings Reservoir, the environment exhibited

a diverse array of hydrodynamic characteristics. This variability permitted thorough monitoring and interpretation across the entire water body, enhancing the robustness of the findings.

2 MATERIALS AND METHODS

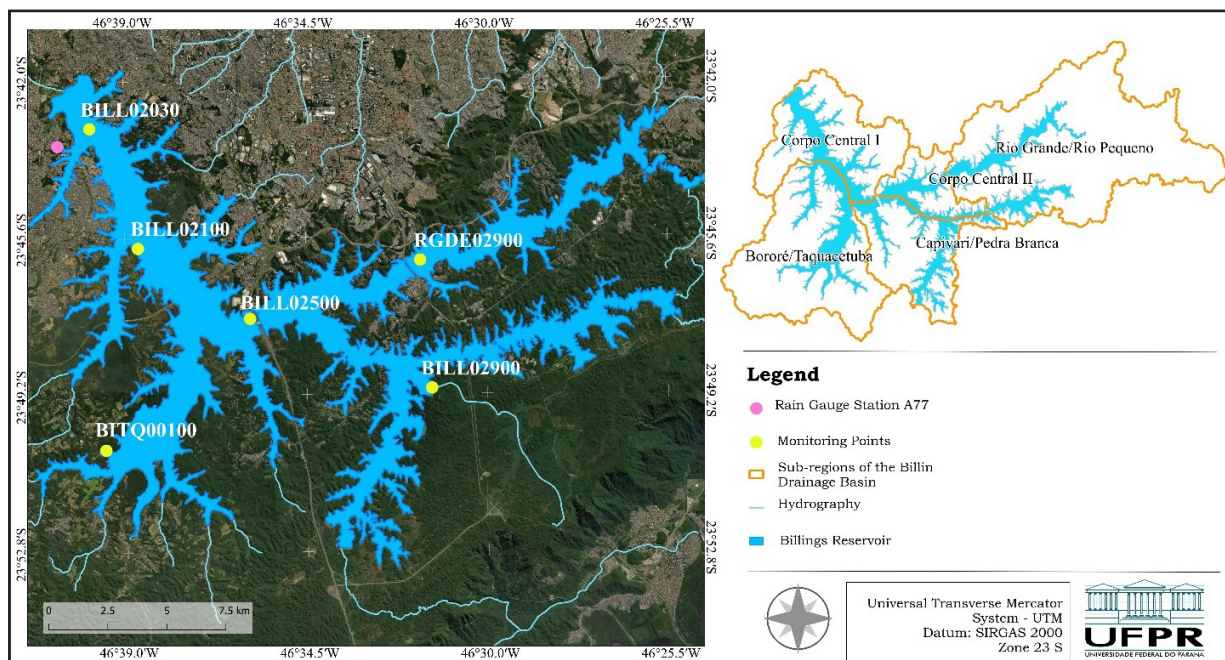
The Billings Reservoir (Figure 1) encompasses a maximum flooded area of 127 km², a storage volume of 1,200 hm³, and an average retention time of 600 days (Amorim 2020). It is characterized by an estimated average natural inflow of 12.5 m³/s and an average depth of 18 m (Amorim 2020). According to studies by Jesus (2006) and Amorim (2020), the Billings Reservoir is divided into eight distinct units, referred to as arms, which contribute to the complexity of its hydrodynamic behavior and water quality characteristics.

Hydrodynamic processes within the Billings Reservoir are influenced by a variety of factors, including energy generation, water pumping from the Pinheiros River, nutrient inflow, and pollution (Jesus 2006; Gargiulo et al. 2022). Moreover, the water body is affected by urban water supply demands, prevailing wind patterns, diffuse pollution sources, and sewage discharge from the surrounding population (Gemelgo et al. 2009; Amorim 2020). These interrelated factors contribute to the reservoir's overall water quality dynamics and highlight the need for integrated management strategies to mitigate adverse environmental impacts.

The monitoring points selected for this study are strategically located throughout the Billings Reservoir and its sub-regions, as detailed below: BILL02030 - situated in the central body sub-region, approximately 15 km from the Pedreira dam; BILL02100 - located near the Pedreira dam and oriented towards the Bororé arm; BILL02500 - positioned beneath the Imigrantes Highway bridge; BILL02900 - found in the Capivari sub-region, adjacent to the Summit Control dam; BITQ00100: - located in the Taquacetuba arm within the Bororé sub-region; and RGDE02900 - situated in the Rio Grande Reservoir, specifically within the public water supply intake region.

The locations of these monitoring points are illustrated in Figure 1. All monitoring sites are part of CETESB's Basic Network, with BILL02900 and BITQ00100 undergoing automatic monitoring. Furthermore, CETESB employs a range of data collection methodologies, encompassing both shoreline sampling and in-water column sampling (CETESB 2011).

Figure 1 – Map of the Billings Reservoir illustrating the monitored points and the sub-regions of the drainage basin, including Central Body I, Central Body II, Bororé/Taquacetuba, Capivari/Pedra Branca, and Rio Grande



Source: the authors (2025)

For satellite image analysis, two tools were utilized: (1) SNAP 8.0.0 software, developed by the European Space Agency, specifically for processing Sentinel images; and (2) the AlgaeMap application, implemented on Google Earth Engine (GEE), which offers interactive functionalities (Lobo et al. 2021). Both tools are designed to process Sentinel-2 satellite images, which are central to this study.

Atmospheric correction in SNAP was conducted using the Case-2 Regional Coast Color (C2RCC) plugin, recognized for its effectiveness in aquatic studies (Pompêo et al. 2019). As highlighted by Pompêo et al. (2021) and Brockmann et al. (2016), the C2RCC

atmospheric correction method employs a neural network trained on a comprehensive database of reflectances and radiative simulations derived from radiative transfer models, specifically utilizing band B1 (443 nm). Following the processing in SNAP, the resulting product included the Chl-a estimated by the model outlined in Brockmann et al. (2016).

AlgaeMap, as outlined by Lobo et al. (2021), employs the Satellite Invariant Atmospheric Correction (SIAC) within GEE. This tool has been calibrated and validated using in situ data collected by the CETESB, which spans from August 2015 to November 2020. For the SNAP analysis, satellite images were selected based on a criterion of cloud cover not exceeding 15%. It is important to note that no specific thresholds for cloud cover were identified in the existing literature.

Consequently, a total of 37 images were processed for the period from January 2017 to December 2021. Among these, only two Sentinel-2 images aligned with the CETESB data collection dates, specifically on May 22, 2019, and May 26, 2021. The remaining images exhibited a temporal gap of 3 to 15 days between the CETESB data collection and the corresponding satellite overpass.

In contrast, AlgaeMap analyzed Sentinel-2 images even when cloud cover reached up to 100%, thereby enabling a greater number of matches with field collection dates. As a result, during the same study period, AlgaeMap processed data from 209 images, whereas SNAP utilized less than 20% of the available images.

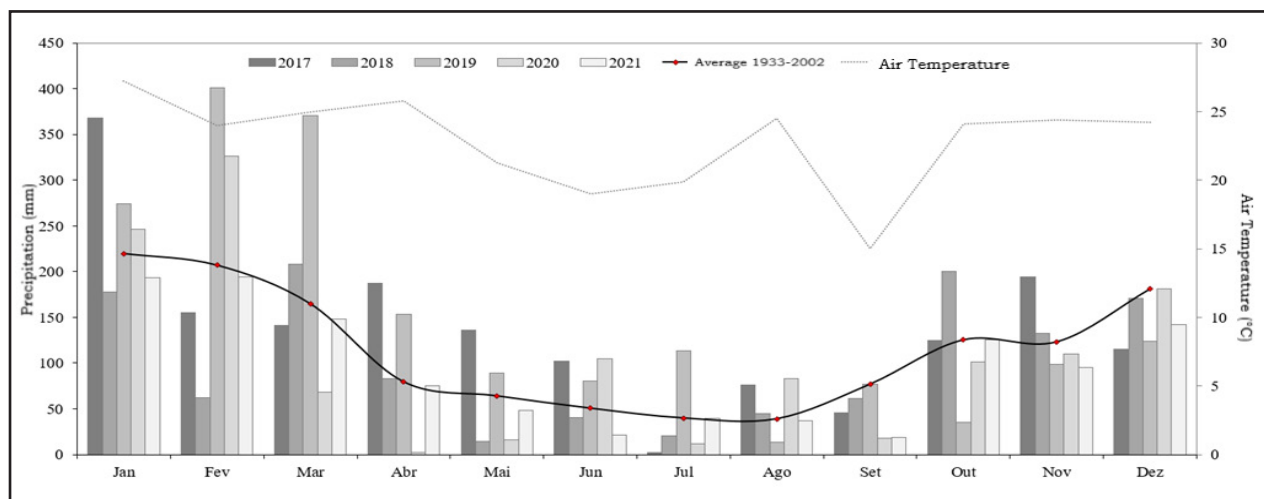
The interpretation of data obtained from these tools was compared against in situ measurements from CETESB, accessible via the InfoÁguas platform (<https://cetesb.sp.gov.br/infoaguas/>), covering the period from 2017 to 2021. This comparison included both temporal and spatial analyses. To assess the strength and direction of the linear relationship between the variables, Pearson correlation was employed as the statistical method.

As proposed by Santos et al. (2018), a coefficient value approaching -1 or 1 indicates a perfect negative or positive correlation, respectively. Conversely, a value of 0 denotes no linear relationship, while intermediate values suggest varying degrees of

partial correlation. To further support the interpretation of results, linear regression analysis was also conducted. According to Cadorin et al. (2023), a linear equation can be derived to predict the dependent variable based on the values of the independent variable.

In a related study, Amorim (2020) developed a water quality assessment project utilizing hydrodynamic modeling through the Delft3D software. The comparison between remotely sensed data and modeled outputs was viable for the monitoring point BILL02030, situated in the upstream region. Still, this comparison was limited to the period for which modeled data was available, specifically from October 2018 to January 2019.

Figure 2 – Historical precipitation series based on rainfall data obtained from the National Institute of Meteorology (INMET) platform (<https://bdmep.inmet.gov.br/>). The data were collected from rain gauge station A771, situated in proximity to the Billings Reservoir



Source: the authors (2025)

For the evaluation of Chl-a, two distinct periods were analyzed: (1) the dry period, encompassing April to September, and (2) the rainy period, spanning October to March. The interpretation of results was grounded in the monthly averages for each year, with the objective of identifying potential monthly similarities. Historical precipitation data

were sourced from the National Institute of Meteorology (INMET), while average air temperature data for the same period were provided by CETESB.

Figure 2 illustrates the precipitation data, emphasizing the maximum rainfall indices across all months of the year along with the corresponding monthly averages. Additionally, the average air temperature data, estimated for the years 2017 to 2021, pertains specifically to the monitoring point RGDE02900 (CETESB).

Analysis of Figure 2 reveals that the rainy season (October to March) is characterized by significantly higher rainfall indices, a trend consistent with historical averages from 1933 to 2002. Differently, the dry season (April to September) experiences markedly lower precipitation levels. Additionally, the air temperature data presented in Figure 2 indicates that higher temperature averages, around 25°C, are observed during the rainy season, aligning with the spring and summer months. Conversely, during the dry season, air temperatures decrease to approximately 20°C.

3 RESULTS

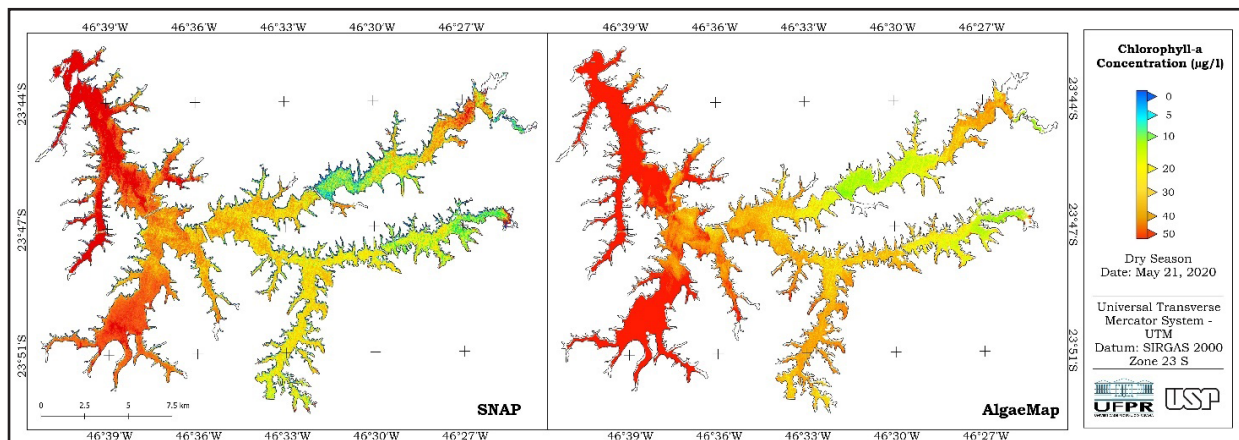
The spatial variation analysis conducted using SNAP and AlgaeMap, as illustrated in Figure 3, revealed comparable results during the dry period. While the initial comparison on May 21, 2020, indicated spatial similarities between the two tools, a more detailed examination uncovered significant quantitative discrepancies. For instance, at the Taquacetuba arm (BITQ00100), AlgaeMap recorded a Chl-a concentration of 71.5 µg/l, whereas SNAP reported only 8.2 µg/l. Similarly, on May 26, 2020, AlgaeMap indicated 96.4 µg/l for the same monitoring point, compared to SNAP's 52.1 µg/l. These findings suggest that the discrepancies in Chl-a values between the two tools do not follow a consistent pattern.

It is important to note that there were no CETESB measurements available for May 21 and May 26, 2020. The closest available measurement was taken on March 5, 2020, which recorded a Chl-a of 55.24 µg/l. While this value aligns more closely with the SNAP data from May 26, it remains unreliable due to the nearly three-month gap.

Without direct measurements during the corresponding dates, it is difficult to validate the remote sensing data.

Conversely, the measurement closest to AlgaeMap's data was taken on March 7, 2020, which indicated a Chl-a concentration of 30.11 µg/l. This value closely approximates the CETESB measurement but still demonstrates a significant difference. Additionally, SNAP did not process any images during March 2020, which means a direct comparison between the satellite imagery and CETESB measurements for that month was not possible.

Figure 3 – Spatial comparison of Chl-a concentrations during the dry period between SNAP (left) and AlgaeMap (right) on May 21, 2020. The colored areas indicate varying concentrations, measured in µg/l, across the Billings Reservoir



Source: the authors (2025)

Upon analyzing the daily data point by point, it was observed that the central body sub-region, particularly the monitoring point BILL02030, exhibited the greatest differences in Chl-a. In contrast, the points BILL02500, BILL02900, and RGDE02900 showed SNAP values that were closer to those recorded by AlgaeMap. On May 21, 2020, for instance, the point BILL02500 displayed remarkably similar Chl-a levels, with AlgaeMap reporting 23.2 µg/l and SNAP recording 22.5 µg/l.

Similarly, in the Rio Grande reservoir (RGDE02900), the Chl-a values remained close for both methodologies, with SNAP indicating 19.2 µg/l and AlgaeMap showing 14.0 µg/l. This suggests that the central monitoring points obtained through SNAP

exhibited a stronger correlation with AlgaeMap compared to the points located at the edges of the reservoir.

This quantitative analysis reinforces the spatial interpretation illustrated in Figure 3, where both AlgaeMap and SNAP yielded similar results in the central region of the reservoir. In the Rio Grande Reservoir, the data from both tools indicated that Chl-a concentrations are lower in the upstream region and progressively increase downstream, as shown in the same figure.

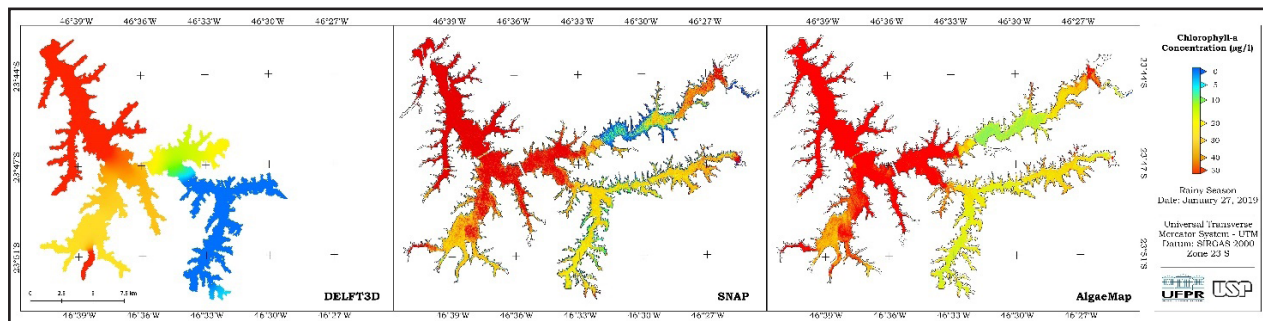
In the analysis of spatial variation during the rainy period, represented by Figure 4 from January 27, 2019, it was noted that AlgaeMap reported higher Chl-a values at the headwaters compared to SNAP. Specifically, at the monitoring point BILL02030, located in the upstream region, AlgaeMap recorded a Chl-a of 374.6 µg/l, while SNAP indicated a value of 265.7 µg/l on the same date. However, the closest measurement conducted by CETESB was on January 22, 2019—just five days prior to the modeled data—where it recorded a significantly higher value of 574.7 µg/l.

This measurement is notably above both the remote sensing data and the modeled value from Delft3D, which was only 49.9 µg/l at that point. The observed decrease in Chl-a values from CETESB to the remote sensing and modelling data may be attributed to several factors, such as temporal variations in algal blooms or differences in measurement techniques and timing (Pompêo et al. 2021; Gurski et al. 2021).

When examining the monitoring point BILL02500, located in the central body of the reservoir, the Chl-a values obtained from both tools were quite similar during the rainy period, mirroring the consistency observed in the dry period. AlgaeMap recorded a Chl-a concentration of 52.4 µg/l, while SNAP indicated a value of 49.2 µg/l.

Contrarily, the measurement taken by CETESB at this monitoring point was significantly lower, at just 16.04 µg/l, suggesting that the remote sensing data may have overestimated the Chl-a compared to field measurements. Additionally, no Delft3D model data was extracted for this point, which hindered the ability to compare the remote sensing results with hydrodynamic modeling.

Figure 4 – Spatial comparison of Chl-a concentrations during the rainy period on January 27, 2019, illustrating the results from Delft3D (left), SNAP (middle), and AlgaeMap (right). The colored areas indicate varying concentrations in $\mu\text{g/l}$ across the Billings Reservoir



Source: the authors (2025)

From Figure 4, it is evident that in the headwater region, all three methodologies (Delft3D, SNAP, and AlgaeMap) displayed similar trends, with elevated Chl-a levels. Alternatively, the Taquacetuba arm recorded lower Chl-a in Delft3D compared to the remote sensing tools. But, in the upstream region of the Rio Grande Reservoir, Delft3D and AlgaeMap yielded comparable results. Notably, at the location of point BILL02900, Delft3D indicated Chl-a values around zero, rendering a comparison with satellite images unfeasible. In this instance, SNAP and AlgaeMap produced similar values.

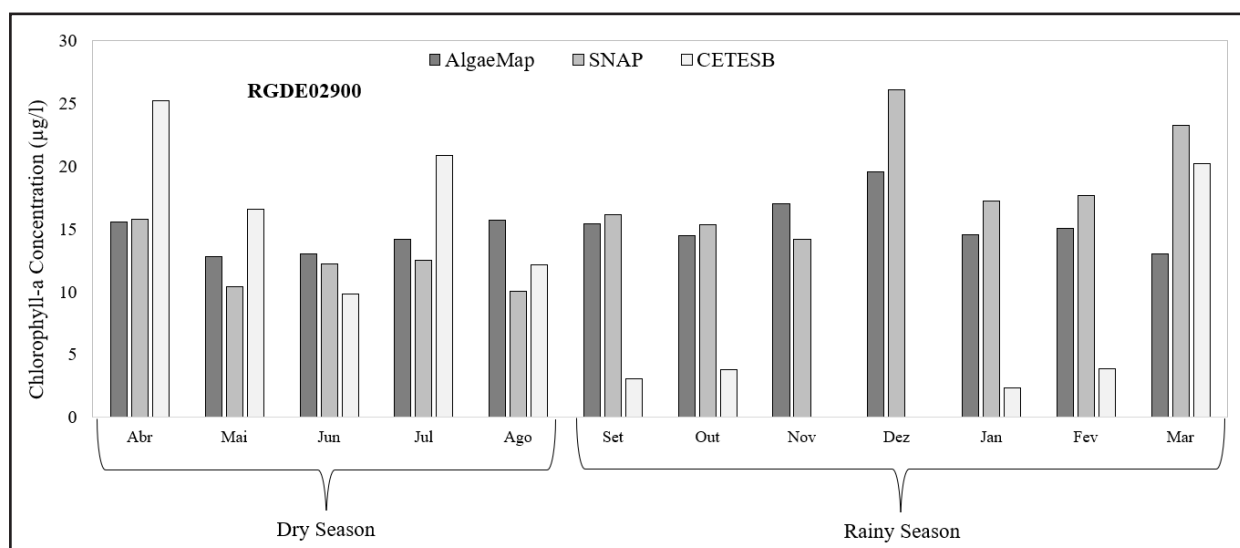
In evaluating the tools SNAP, AlgaeMap, and Delft3D alongside precipitation data, it was observed that during the dry months, characterized by low rainfall, there was a corresponding decrease in Chl-a levels. For instance, in June 2018, which recorded 40.2 mm of rain, the monthly average Chl-a concentration was 39 $\mu\text{g/l}$ according to SNAP, while AlgaeMap reported a slightly higher value of 50 $\mu\text{g/l}$. Conversely, an increase in precipitation was associated with a rise in Chl-a levels.

Additionally, the analysis of the last three months of the evaluated period (November 2018, December 2018, and January 2019) revealed that November exhibited the closest agreement, with an average monthly concordance of 2.15% between AlgaeMap and CETESB, making it the best match among the three months. In December, the agreement rate between the remote sensing tools and the modeled data increased to 10.84%.

However, in January 2019, a significant discrepancy emerged, with Delft3D reporting a Chl-a of 49.9 µg/l while AlgaeMap indicated a much higher value of 257.8 µg/l. When comparing SNAP and Delft3D for January, the proximity rate was 67.13%, indicating a substantial difference between the modeled and orbital data.

In the analysis of the monthly averages for the RGDE02900 monitoring point (Figure 5), it was noted that, on the other hand to the upstream points in the Billings Reservoir, which exhibited Chl-a exceeding 100 µg/l, the Chl-a values in the Rio Grande Reservoir remained below 30 µg/l. Furthermore, the Pearson correlation analysis for this monitoring point indicated a moderate correlation between SNAP and AlgaeMap, yielding a coefficient of 0.46.

Figure 5 – Monthly average Chl-a concentrations at monitoring point RGDE02900, located at the water intake, from 2017 to 2021



Source: the authors (2025)

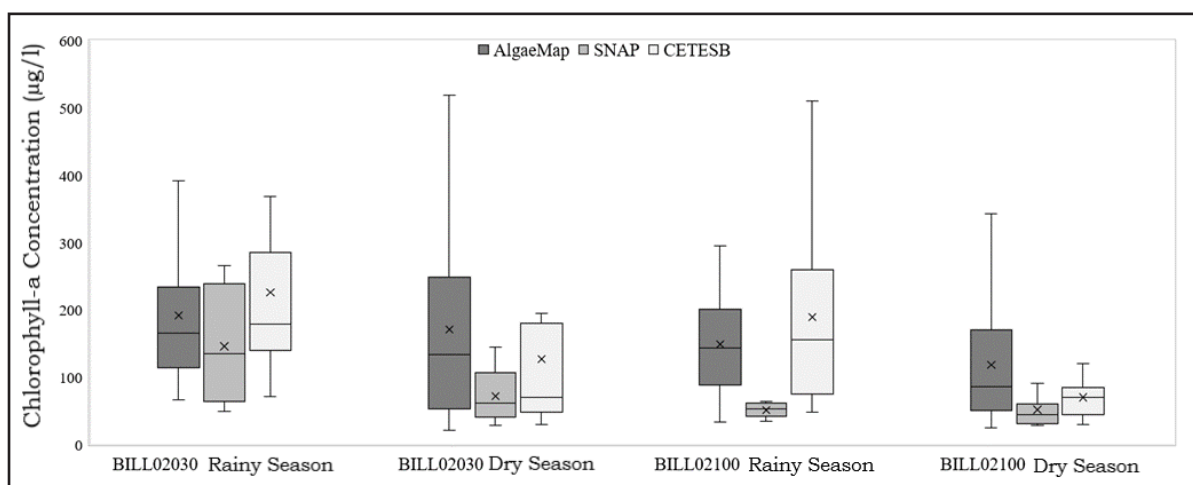
Additionally, a moderate negative correlation was observed between the orbital data and the field measurements. Notably, the correlation between AlgaeMap and CETESB (-0.21) was stronger than that between SNAP and CETESB (-0.05). Figure 5 further illustrates that, generally, during the dry period, remote sensing tools tend to underestimate in situ data, whereas in the rainy period, they tend to overestimate field

data. Nonetheless, it's important to highlight that in some months of the rainy season, field data were not collected, which limits the ability to confirm whether remote sensing consistently overestimates in situ measurements throughout all months.

Figure 6 presents the boxplot results for two monitoring points in the central body sub-region of the Billings Reservoir, identified as BILL02030 and BILL02100. When analyzing the point BILL02030 during the dry period, it was noted that the medians for SNAP and CETESB were relatively close. However, the Pearson correlation between these two tools was low, at 0.26. In contrast, during the rainy period, the median value of AlgaeMap was closer to that of CETESB, resulting in a higher Pearson correlation of 0.64.

Regarding the monitoring point BILL02100, during the dry period, the median value from AlgaeMap was closer to that of CETESB, with a correlation of 0.52 between the two. In the rainy period, both the median and mean values of AlgaeMap approached those of CETESB, resulting in a correlation of 0.61. Analyzing the correlation matrices across all monitoring points, it was observed that relationships exceeding 0.70 occurred during the dry period. Specifically, for BILL02030, the correlation between AlgaeMap and SNAP was 0.75, while for BILL02100, the correlation between SNAP and CETESB reached 0.88.

Figure 6 – Boxplot comparing SNAP, AlgaeMap, and CETESB methodologies during the dry and rainy periods for monitoring points BILL02030 and BILL02100, covering the years 2017 to 2021



Source: the authors (2025)

When analyzing two additional monitoring points—one in the Taquacetuba sub-region (BIT00100) and another in the Capivari sub-region (BILL02500)—it was found that during the dry period, the median Chl-a reported by CETESB at BIT00100 was lower than that of AlgaeMap. The Pearson correlation coefficients for this period were weak: 0.27 for the relationship between AlgaeMap and CETESB, and 0.29 for SNAP and CETESB.

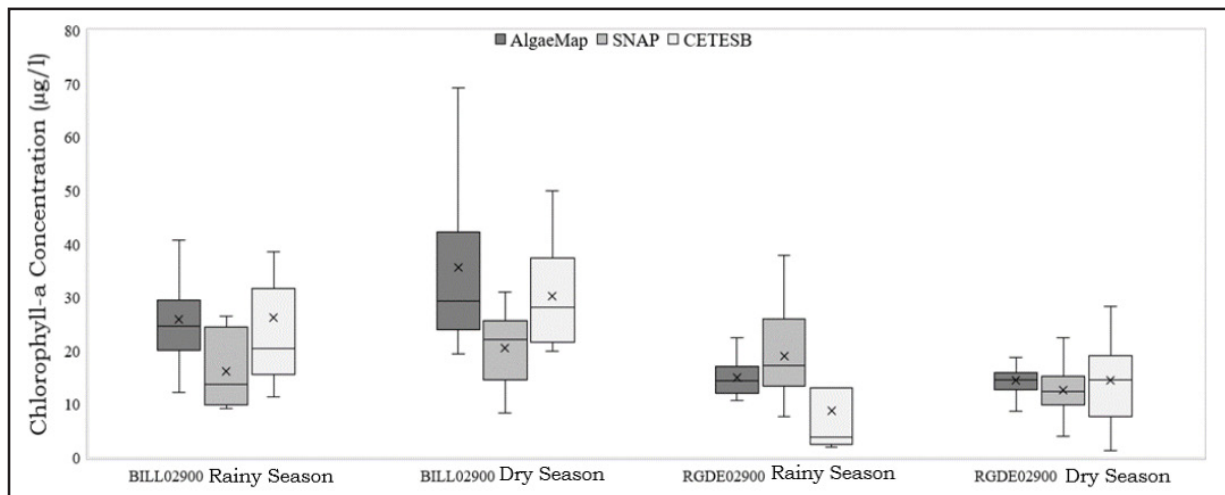
In opposition, at BILL02500 during the dry period, the median and mean Chl-a values for AlgaeMap and CETESB were similar, resulting in a Pearson correlation of 0.61. During the rainy period, CETESB's mean value exceeded that of AlgaeMap, causing the correlation to drop to 0.12. Notably, the strongest correlations between the two remote sensing tools were observed at BILL02500 in both periods, with values of 0.72 in the dry period and 0.78 in the rainy period.

Figure 7 illustrates the monitoring points in Capivari (BILL02900) and the Reservoir Rio Grande (RGDE02900). Analyzing BILL02900 individually, it was found that during the dry period, the median and mean Chl-a values for AlgaeMap and CETESB were very similar, resulting in a Pearson correlation of 0.47. Conversely, during the rainy period, AlgaeMap's median was higher than that of CETESB, leading to a correlation of -0.50.

For the monitoring point RGDE02900, both the median and mean values of Chl-a from AlgaeMap and CETESB were similar during the dry period. SNAP also displayed mean and median values close to those of CETESB. The Pearson correlation for this period revealed a weak correlation in magnitude, with AlgaeMap and CETESB at -0.004, indicating a relationship closer to zero.

During the rainy period for RGDE02900, the mean and median values of Chl-a from AlgaeMap and SNAP were similar, with a Pearson correlation of -0.17 between the two remote sensing tools. However, separate analyses revealed that AlgaeMap and CETESB exhibited a correlation of -0.42, while SNAP and CETESB demonstrated a strong correlation of 0.96.

Figure 7 – Boxplot comparing Chl-a values during dry and rainy periods across different methodologies (SNAP, AlgaeMap, and CETESB) for monitoring points BILL02900 and RGDE02900 from 2017 to 2021



Source: the authors (2025)

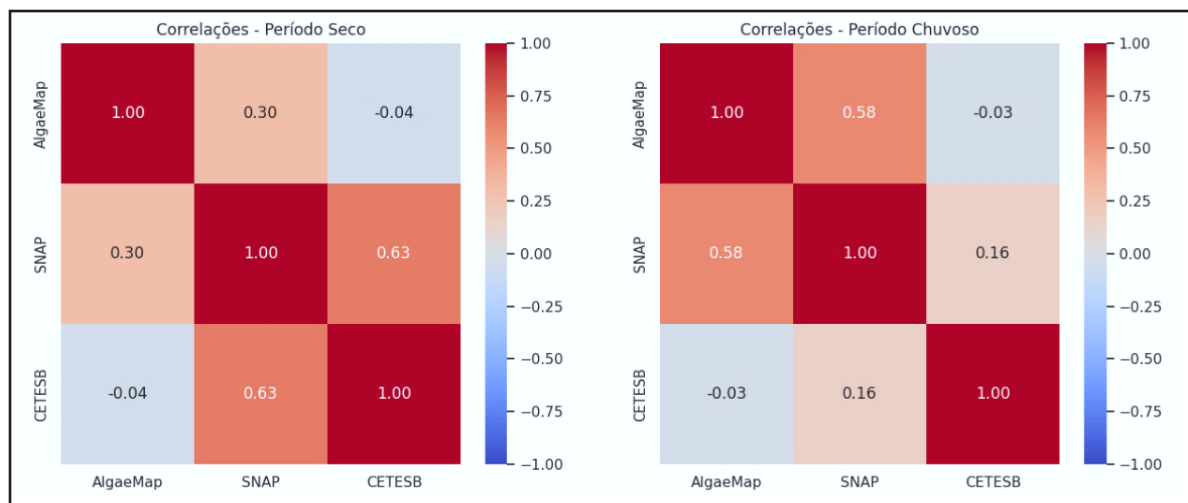
The Pearson correlation analysis, encompassing all monitoring points and dates evaluated, is presented in Figure 8. The results indicate a moderate positive correlation between AlgaeMap and SNAP during the rainy period, suggesting a significant association between these two variables. This finding implies that as AlgaeMap values increase, SNAP values also tend to rise, and vice versa, though the relationship is not perfectly linear. Conversely, the correlation between AlgaeMap and CETESB was found to be virtually zero (-0.03), indicating a lack of linear relationship between these two variables during the rainy period.

Furthermore, Figure 8 illustrates the correlation behavior during the dry period, revealing distinct patterns among the AlgaeMap, SNAP, and CETESB variables compared to the rainy period. While the correlation between AlgaeMap and SNAP remains positive, indicating some level of association, its magnitude significantly decreases to 0.30, suggesting a less robust relationship during the dry period.

In contrast, the correlation between SNAP and CETESB increases substantially to 0.63, indicating a strong positive association between these variables. The correlation

between AlgaeMap and CETESB remains close to zero, reflecting an absence of a linear relationship during the dry period, consistent with the findings from the rainy period.

Figure 8 – Pearson correlation analysis for all monitoring points across the three methodologies: SNAP, AlgaeMap, and CETESB during the years 2017 to 2021. The left side displays correlations for the dry season, while the right side illustrates correlations for the rainy season



Source: the authors (2025)

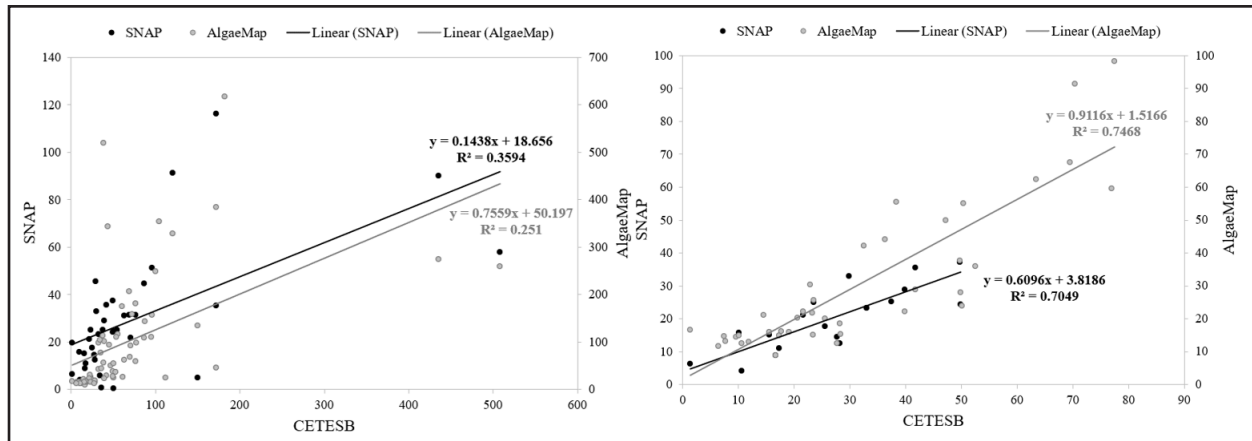
In the linear regression analysis between SNAP and CETESB, as illustrated in Figure 9, the coefficient of determination (R^2) was found to be 0.36 for the dry period. In comparison, the linear regression between AlgaeMap and CETESB yielded an R^2 of 0.25 for the same timeframe.

Notably, a closer examination revealed that both SNAP and AlgaeMap data were more aligned with CETESB values when Chl-a were limited to 100 $\mu\text{g/l}$. Based on this observation, data points with Chl-a values exceeding this threshold were excluded to better evaluate the relationship between the datasets under this condition.

After applying this exclusion, the analysis in Figure 9 (right side) revealed that the R^2 for SNAP increased to 0.71, while the R^2 for AlgaeMap rose to 0.75 in relation to CETESB data. This adjustment demonstrated a significant enhancement

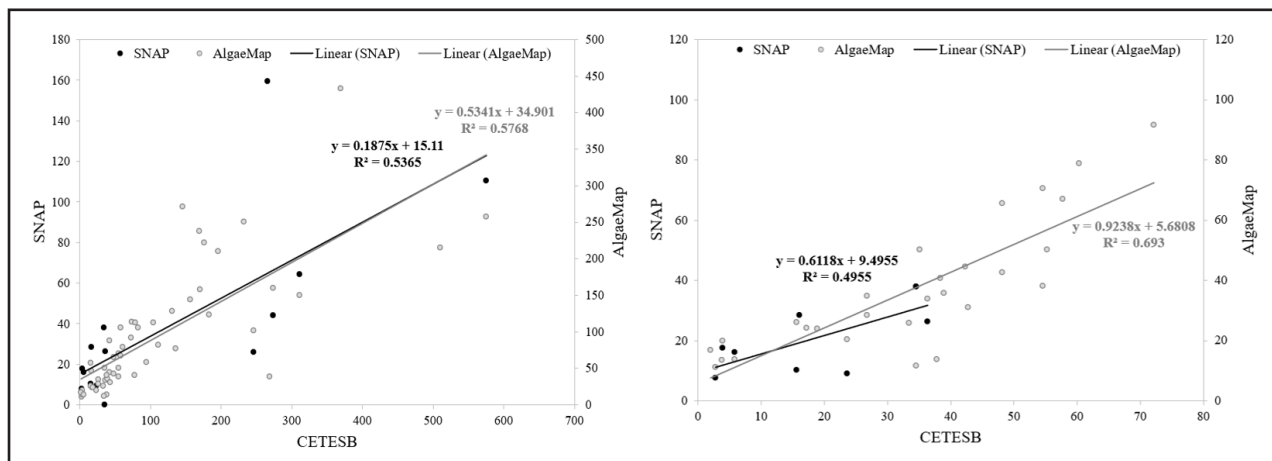
in the correlation between Chl-a values obtained through SNAP and AlgaeMap when considering only data below 100 µg/l.

Figure 9 – Linear regression analysis for the dry period (April to September) comparing SNAP and CETESB, as well as AlgaeMap and CETESB, across all monitoring points from 2017 to 2021. Left: All data. Right: Data limited to Chl-a values up to 100 µg/l



Source: the authors (2025)

Figure 10 – Linear regression analysis for the wet period (October to March) comparing SNAP versus CETESB and AlgaeMap versus CETESB across all monitoring points from 2017 to 2021. The left side displays results using all data, while the right side focuses on data with Chl-a values up to 100 µg/l

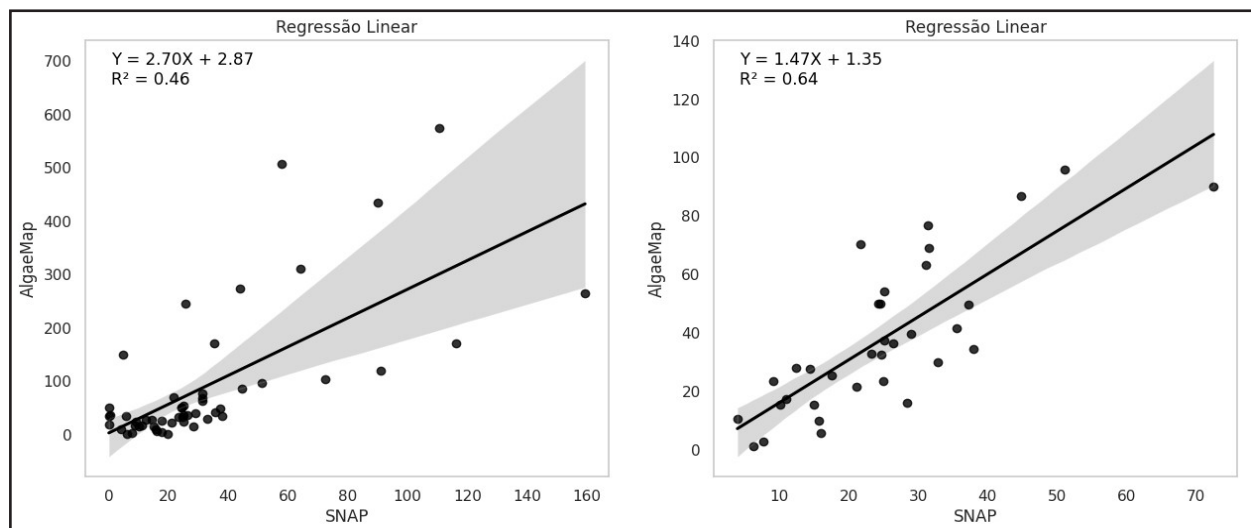


Source: the authors (2025)

Figure 10 presents the results for the wet period. Analyzing data from all monitoring points, the coefficient of determination for the correlation between SNAP and CETESB was 0.54, while for AlgaeMap and CETESB, it was 0.58. Both correlations indicate a moderate relationship, suggesting that while the results are associated, they are not strongly interlinked.

Applying the 100 µg/l Chl-a restriction revealed that SNAP exhibited a weaker relationship with CETESB, yielding an R^2 of 0.50, while AlgaeMap showed a stronger association with an R^2 of 0.69. Thus, during the wet period, AlgaeMap provided better results under this Chl-a limit, whereas SNAP showed minimal change.

Figure 11 – Linear regression analysis comparing SNAP and AlgaeMap methodologies across all monitoring points from 2017 to 2021. Left side: All data. Right side: Data limited to chlorophyll-a concentrations up to 100 µg/l



Source: the authors (2025)

Figure 11 shows the linear relationship between the two remote sensing tools (SNAP and AlgaeMap), as both use the same satellite to assess chlorophyll-a concentration. Analysis of all monitoring points reveals that the relationship between AlgaeMap and SNAP had a coefficient of determination of 0.46, indicating a weak relationship between the variables.

When restricting the chlorophyll-a value to 100 µg/l, the relationship between SNAP and AlgaeMap improved, yielding a coefficient of determination of 0.64 across all monitoring points. This increase in R^2 indicates a more robust association between the two tools when evaluating specific chlorophyll-a concentrations, offering a more accurate perspective on the relationship between SNAP and AlgaeMap under these restricted conditions.

3 CONCLUSIONS

The processing capabilities of SNAP are heavily dependent on the availability of cloud-free images, leading to notable discrepancies in the volume of data processed compared to AlgaeMap, which utilizes all images captured within a 5-day recurrence interval (Lobo et al. 2021). While both analyses reveal moderate correlations between variations, the limited number of observations available for SNAP may influence the reliability of the results.

Although both SNAP and AlgaeMap utilize the same satellite, AlgaeMap—calibrated with CETESB data—showed a closer alignment with actual field measurements. On the other hand, SNAP has demonstrated its ability to operate effectively without field data for calibration when using the C2RCC methodology. However, the lack of available field data during certain months significantly affected the evaluation of the relationship between remote sensing and in situ measurements over the entire study period.

The monitoring point RGDE02900 demonstrated the strongest relationship between the remote sensing methodologies. According to Jesus (2006), the construction of the Anchieta Dam in 1982 separated the Rio Grande Reservoir from the Billings Reservoir to facilitate the capture of raw water for the water treatment station. In the Rio Grande, algicides are employed to inhibit algal growth (Jesus 2006), which explains why chlorophyll-a levels at RGDE02900 consistently remain below 30 µg/l, while levels in the Billings headwaters region exceed 100 µg/l.

The Taquacetuba arm (BITQ00100) demonstrated a less consistent relationship. Notably, the C2RCC atmospheric correction exhibited failures for high Chl-a, particularly in the headwater's region of the reservoir during the rainy season. These inconsistencies may be attributed to environmental and temporal conditions that cause variations in Chl-a levels.

If the model does not adequately account for these fluctuations, its predictions may be compromised. Furthermore, changes in water quality—such as the presence of other substances that affect light absorption—can also influence Chl-a detection, potentially leading to failures in the neural network model (Pompêo et al. 2019).

The failures in the SNAP methodology led to insufficient data in the upstream region of the reservoir, which directly impacted data collection at the BILL02030 monitoring point. Moreover, the proximity of the BITQ00100 monitoring point to the reservoir's edge may have influenced the average pixel values in SNAP. This proximity could result in the inclusion of edge pixels, which may have further affected the SNAP results and contributed to the observed discrepancies.

Interpreting the correlation between the methodologies SNAP, AlgaeMap, Delft3D, and CETESB proved challenging due to the limited data and the relatively short study period (October 2018 to January 2019), which encompassed only the rainy season. Nevertheless, the results for AlgaeMap, Delft3D, and CETESB were generally consistent during the evaluated months. An exception occurred in January 2019, when the mathematical model reported Chl-a levels that were lower than those observed in the field and detected by remote sensing.

Linear regression analyses across all monitoring points revealed that SNAP results were more closely aligned with CETESB during the dry period, similar to AlgaeMap's alignment with CETESB. The correlations among SNAP, AlgaeMap, and CETESB data exhibited varied associations. Notably, a strong correlation was observed between SNAP and CETESB during the dry period; but, the relationship between AlgaeMap and CETESB was even stronger during the same timeframe, underscoring the necessity

for a more refined approach in using SNAP. Additionally, applying specific Chl-a limits significantly improved the agreement between the two tools.

Analysis of the relationship between precipitation and Chl-a revealed that during the rainy periods (summer), there is a notable increase in Chl-a levels, indicating a higher presence of phytoplankton. This phenomenon has been documented in studies by Machado and Baptista (2016) and Arraut et al. (2005). Furthermore, the rise in surface water temperature during the summer, coupled with the influx of nutrients and organic matter due to increased rainfall, significantly contributes to the elevation of Chl-a concentrations, as highlighted by Amorim (2020).

Analysis of the relationship between precipitation and Chl-a revealed that, during the rainy periods (summer), there is a higher concentration of Chl-a, indicating increased phytoplankton presence, as addressed in studies by Machado and Baptista (2016) and Arraut et al. (2005). Additionally, the increase in surface water temperature during summer and the influx of nutrients and organic matter related to increased rainfall result in a significant rise in Chl-a, as stated by Amorim (2020).

In conclusion, remote sensing methodologies, whether through AlgaeMap or SNAP, have demonstrated effectiveness in assessing Chl-a in the Billings Reservoir, offering valuable information for watershed management. The observed variations in correlations emphasize the significant impact of seasonal factors and highlight the necessity for tailored approaches that consider the specific characteristics of different periods, monitoring points, and methodologies.

ACKNOWLEDGEMENTS

Brenda Ferreira expresses her gratitude to the Fundação Araucária for the financial support provided during this project. Tobias Bleninger acknowledges the productivity grant from the Conselho Nacional de Desenvolvimento Científico e Tecnológico (CNPq), grant no. 312211/2020-1, reference no. 09/2020.

REFERENCES

Amorim, L. 2020. *Hidrodinâmica e avaliação da qualidade da água de lagos por comportamento térmico e modelagem*. Universidade de São Paulo, São Paulo. Teses, p. 155.

Barbosa, C. C. F.; Novo E. M. L. M.; Martins, V. S. 2019. *Introdução ao sensoriamento remoto de sistemas aquáticos: princípios e aplicações*. Instituto Nacional de Pesquisas Espaciais, São José dos Campos, p. 161.

Brockmann, C.; Doerffer, R.; Peters, M.; Stelzer, K.; Embacher, S.; Ruescas, A. 2016. *Evolução da rede neural C2RCC para Sentinel 2 e 3 para a recuperação de produtos de cor oceânica em águas normal e extremamente ópticas complexas*. Disponível em: http://step.esa.int/docs/extra/Evolution%20of%20the%20C2RCC_LPS16.pdf.

Cadorin, G. R., Destefani, A., Martins, C. E. N.; Souza, A. L. F. 2023. Parâmetros significativos para monitoramento e avaliação da qualidade da água, Bacia Hidrográfica do Rio Cachoeira (Joinville, Santa Catarina, Brasil). *Rev. Gest. Água Am. Lat.*, Porto Alegre, v. 20, e14.

Companhia Ambiental do Estado de São Paulo. 2011. *Guia nacional de coleta e preservação de amostras: água, sedimento, comunidades aquáticas e efluentes líquidos*. Organizadores: Carlos Jesus Brandão, Marcia Janete Coelho Botelho, Maria Inês Zanolli Sato, Marta Condé Lamparelli, et al. São Paulo: CETESB; Brasília: ANA. 326 p.: il.

Gargiulo, J. R. B. C.; Pompêo, M. L. M.; Cardoso-Silva, S.; Petesse, M. L.; Menezes, L. C. B. 2022. Compartimento Taquacetuba do Reservatório Billings (SP, Brasil): influência diferencial do corpo de água central e dos tributários na qualidade da água. *Acta Limnologica Brasiliensis*, vol. 34, e4.

Gemelgo, M. C. P., Mucci, J. L. N.; Navas-Pereira, D. 2009. Dinâmica populacional: variação sazonal de grupos funcionais de fitoplâncton em reservatórios brasileiros (Billings e Guarapiranga, São Paulo). *Brazilian Journal of Biology*, v. 69, p. 1001-1013.

Gurski, L. K. K., Lisboa, L. A., Ishikawa, M. M., Knapik, H. G., Prado, L. L., Bleninger, T.; Scheer, M. B. 2021. Monitoramento mínimo do parâmetro clorofila a em um reservatório mesotrófico de água potável a partir de medições realizadas por sensor com tecnologia espectral. *XXIV Simpósio Brasileiro de Recursos Hídricos* (ISSN 2318-0358).

Jesus, J. A. O. 2006. *Utilização de modelagem matemática 3D na gestão da qualidade da água em mananciais – aplicação no reservatório Billings*. São Paulo: Tese de Doutorado – Universidade de São Paulo (USP), p. 150.

Lobo, F. d. L., Nagel, G. W., Maciel, D. A., Carvalho, L. A. S. d., Martins, V. S., Barbosa, C. C. F.; Novo, E. M. L. d. M. 2021. AlgaeMAP: Algae Bloom Monitoring Application for Inland Waters in Latin America. *Remote Sensing*, 13, 2874.

Machado, M. T. de S.; Baptista, G. M. de M. 2016. Sensoriamento remoto como ferramenta de monitoramento da qualidade da água do Lago Paranoá (DF). *Engenharia Sanitária e Ambiental*, v. 21, n. 2, p. 357-365.

Neves, V. H., Pace, G., Delegido, J.; Antunes, S. C. 2021. Chlorophyll and Suspended Solids Estimation in Portuguese Reservoirs (Aguieira and Alqueva) from Sentinel-2 Imagery. *Water*, 13(18), 2479.

Pompêo, M.; Moschini-Carlos, V.; Bitencourt, M.D.; Sòria-Perpinyà, X.; Vicente, E.; Delegido, J. 2021. Avaliação da qualidade da água usando imagens Sentinel-2 com estimativas de clorofila a profundidade do disco de Secchi e número de células de cianobactérias: os reservatórios do Sistema Cantareira (São Paulo, Brasil). *Environmental Science and Pollution Research*, v. 28, p. 34990-35011.

Pompêo, M.; Sòria-Perpinyà, X.; Soria Garcia, J. M.; Delegido, J.; Urrego, E. P.; Pereira-Sandova, M.; Vicente, E. 2019. *Sentinel 2 (A e B): protocolo de instalação e uso para trabalhar imagens na avaliação da qualidade da água de reservatórios*. São Paulo: Instituto de Biociências, 38 p. ISBN 978-85-85658-78-6

Santos, S. A.; Gastaldini, M. C. C.; Pivetta, G. G.; Schmidt Filho, O. 2018. Qualidade da água na bacia hidrográfica urbana Cancela Tamandai, Santa Maria/RS. *Soc. Nat.*, Uberlândia, MG, v.30, n.2, p.23-44, mai./ago. 2018, ISSN 1982-4513.

SNAP. 2022. *Sentinel Application Platform*. Agência Espacial Europeia. Disponível em: <https://earth.esa.int/eogateway/tools/snap>. Acesso em: 30 Out 2022.

Authorship contributions

1 – Brenda Camila Ferreira

Master's Degree Student at Federal University of Paraná
<https://orcid.org/0009-0005-2917-7680> - brendacamila@ufpr.br
Contribution: Writing - original draft

2 – Tobias Bleninger

Professor at Federal University of Paraná
<https://orcid.org/0000-0002-8376-3710> - bleninger@ufpr.br
Contribution: RReview & editing

3 – Mayra Ishikawa

Postdoctoral Researcher at The Federal Institute of Hydrology (Germany)
<https://orcid.org/0000-0001-6680-1570> - mayraishikawa@gmail.com
Contribution: Review & editing

4 – José Antônio de Jesus

Postdoctoral Researcher at Federal University of Paraná
<https://orcid.org/0000-0002-6134-1509> - tonico.oj@gmail.com
Contribution: Review & editing

5 – Laís Amorim

Postdoctoral Researcher at University of São Paulo
<https://orcid.org/0000-0003-0127-2553> - amorimlaais8@gmail.com
Contribution: Review & editing

How to quote this article

Ferreira, B. C., Bleninger, T., Ishikawa, . M., Jesus, J. A. de, & Amorim, L. (2025). Comparative analysis of methodologies for assessing chlorophyll-a concentration in the Billings Reservoir. *Ciência e Natura*, Santa Maria, v. 47, spe. 2, e91411. DOI: <https://doi.org/10.5902/2179460X91411>.